Bioorganic & Medicinal Chemistry Letters 23 (2013) 1974–1977

Contents lists available at SciVerse ScienceDirect

Bioorganic & Medicinal Chemistry Letters

journal homepage: www.elsevier.com/locate/bmcl

Discovery of 4-alkylamino-7-aryl-3-cyanoquinoline LRRK2 kinase inhibitors

Albert W. Garofalo [a,*], Marc Adler [b], Danielle L. Aubele [a], Elizabeth F. Brigham [c], David Chian [c], Maurizio Franzini [a], Erich Goldbach [d], Grace T. Kwong [c], Ruth Motter [c], Gary D. Probst [a], Kevin P. Quinn [d], Lany Ruslim [e], Hing L. Sham [a], Danny Tam [e], Pearl Tanaka [c], Anh P. Truong [a], Xiaocong M. Ye [a], Zhao Ren [e]

[a] Department of Medicinal Chemistry, Elan Pharmaceuticals, 180 Oyster Point Blvd., South San Francisco, CA 94080, United States
[b] Department of Molecular Design, Elan Pharmaceuticals, 180 Oyster Point Blvd., South San Francisco, CA 94080, United States
[c] Department of Pharmacology, Elan Pharmaceuticals, 180 Oyster Point Blvd., South San Francisco, CA 94080, United States
[d] Department of Drug Metabolism and Pharmacokinetics, 180 Oyster Point Blvd., South San Francisco, CA 94080, United States
[e] Department of Assay Development, Elan Pharmaceuticals, 180 Oyster Point Blvd., South San Francisco, CA 94080, United States

ARTICLE INFO

Article history:
Received 14 November 2012
Revised 2 February 2013
Accepted 7 February 2013
Available online 15 February 2013

Keywords:
Lrrk2
Leucine-rich repeat kinase 2
Parkinson's disease

ABSTRACT

Mutations in leucine-rich repeat kinase 2 (LRRK2) are associated with familial Parkinson's disease (PD). The kinase activity of this complex protein is increased by pathogenic mutations. Inhibition of LRRK2 kinase activity has therefore emerged as a promising approach for the treatment of PD. Herein we report our findings on a series of 4-alkylamino-7-aryl-3-cyanoquinolines that exhibit kinase inhibitory activity against both wild type and G2019S mutant LRRK2. Activity was determined in both biochemical and cellular assays. Compound **14** was further evaluated in an in vivo pharmacodynamic study and found to significantly inhibit Ser935 phosphorylation after oral dosing.

Parkinson's disease (PD) is a progressive neurological movement disorder affecting 1–2% of the population over the age of 60 and up to 4% over the age of 80.[1,2] In the United States alone it is estimated that there are about 50,000 new cases reported annually and this number is expected to grow as life expectancy increases.[3] Current standards of care have serious limitations and/or drawbacks and largely address only symptoms.[4] Because of these shortcomings there is a clear need for improved therapies.

While most occurrences of PD are sporadic, the discovery of causal mutations in familial forms of PD has opened numerous avenues of investigation. Mutations in leucine-rich repeat kinase 2 (LRRK2) are known to cause autosomal-dominant parkinsonism.[5] There are at least five pathogenic mutations in LRRK2 that have been identified and, of those, the G2019S mutation is the most prevalent amino acid substitution.[6] This mutation is found in the kinase domain of LRRK2 and is reported to cause an increase in kinase activity.[7–9] This enhanced activity suggests that small molecule LRRK2 kinase inhibitors may lead to new PD therapeutics.

We employed a kinase inhibitor-focused screen that identified quinoline amides as hits of which the most potent was compound **1** (Table 1). This screen used an HTRF (homogeneous time-resolved fluorescence) assay measuring the inhibition of LRRKtide phosphorylation.[10] Compounds of this chemotype are known inhibitors of CSF1R as well as PDE4 and we were therefore interested in modifying this hit scaffold.[11,12] We also observed that these quinoline amides have poor CNS penetrance ($B/P = 0.1$ for

Table 1
Initial screening hit and amide replacements

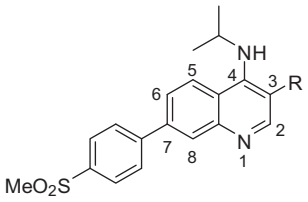

Compound	R	LRRK2 (wt) IC_{50} (μM)	LRRK2 (G2019S) IC_{50} (μM)
1	$CONH_2$	0.039	0.041
2	Acetyl	0.066	0.071
3	Thiazol-2-yl	1.747	2.893
4	4,5-Dihydro-1*H*-imidazol-2-yl	91.856	88.597
5	1-Methyl-1*H*-pyrazol-4-yl	2.020	2.229
6	CN	0.031	0.028

* Corresponding author.
E-mail address: albertwgarofalo@gmail.com (A.W. Garofalo).

0960-894X/$ - see front matter © 2013 Elsevier Ltd. All rights reserved.
http://dx.doi.org/10.1016/j.bmcl.2013.02.041

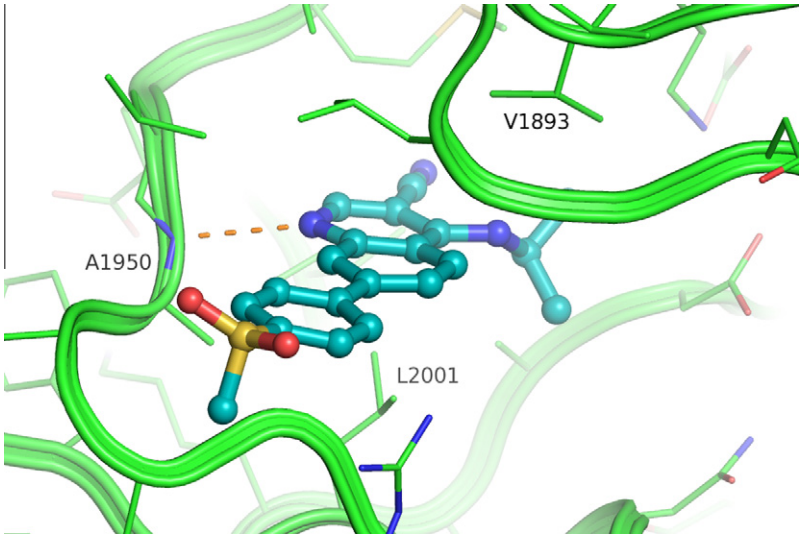

Figure 1. A model of the complex between compound **6** and LRRK2.

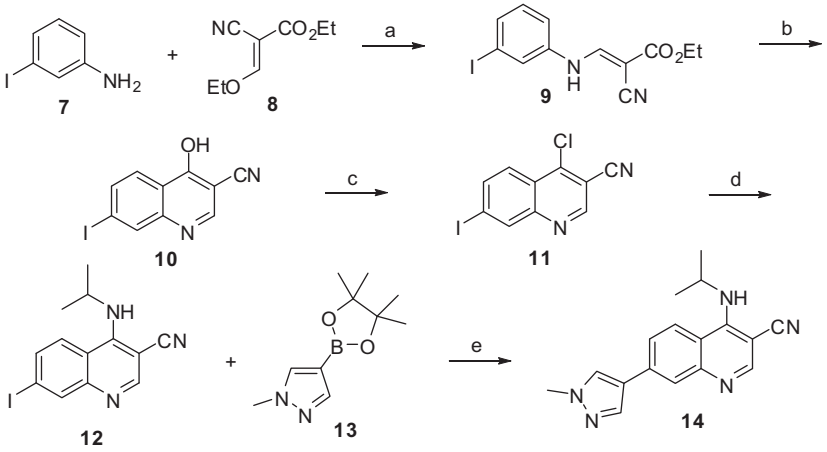

Scheme 1. Reagents and conditions: (a) neat, 120 °C (98%); (b) Dowtherm, reflux; (c) $POCl_3$, reflux (43%, 2 steps); (d) isopropylamine, DMA, 100 °C (76%); (e) $Pd(PPh_3)_4$, K_2CO_3, dioxane, H_2O (67%).

1) and significant P-gp mediated efflux (in vitro efflux ratio = 6.2 for **1**). We ascribed this poor uptake and high efflux to the presence of the amide substituent which led to the search for suitable replacements as listed in Table 1. A twofold loss in potency was the result of replacing the amide with an acetyl group (compound **2**) and much larger decreases in activity were observed with all heterocyclic replacements examined (e.g., **3**, **4**, and **5**). However, incorporation of a nitrile at C3 afforded a compound **6**, that was at least equipotent to the screening hit.

We developed a homology model for LRRK2 based on the crystal structure of mixed-lineage kinase MLK1 (pdb code: 3DTC).[13,14] Compound **6** was docked into our model and showed a hinge binding interaction between the quinoline nitrogen and the A1950 amide (Fig. 1). In this model the methylphenylsulfone is oriented toward the solvent channel and the isopropylamine occupies space between V1893 on the P-loop and L2001 in the C-terminal domain.

Encouraged by the activity of **6** we set about making a number of 3-cyanoquinolines. Taking into consideration the binding mode from our model, we opted to make a set of compounds that were diversified at C4 and C7. These compounds were generally prepared as depicted in Scheme 1. Addition of 3-iodoaniline (**7**) to ethyl 2-cyano-3-ethoxyacrylate (**8**) afforded cyanoacrylate **9**. Thermal cyclization followed by chlorination using $POCl_3$ gave the 4-chloro-7-iodoquinoline **11**. Treatment of **11** with an appropriate amine in DMA followed by Suzuki coupling to C7 provided the desired analogs.

Compound potency was measured in both biochemical and cellular assays and results are reported in Table 2. The in vitro potencies of compounds maintaining the C4 isopropylamino group and varying substitution at C7 (**6**, **14–22**) were not greatly different. However, comparisons with the C7 unsubstituted quinoline, **22**, indicate a clear potency advantage for compounds with substitution at this position. Several analogs with tertiary amine substitution at C4 were prepared (**23–26**). Compounds **23**–**25** exhibited slightly improved potency over the screening hit, **6**, whereas **26** containing a slightly larger, more lipophilic 3° amine, was approximately equipotent. Overall, the data in Table 2 show an increase in biochemical potency with increasing amine basicity; the most potent compounds as measured in the biochemical assays also contain the most basic amine substitution at C4. We have previously reported on a series of cinnoline amides that demonstrated improved potency by changing the C4 isopropylamine to (*R*)-1-cyclopropylethylamine,[15] however, the same benefit was not realized in this series (cf. **6** and **31**, **32**).

Table 2
Inhibitory activity against wild type (wt) and mutant G2019S LRRK2

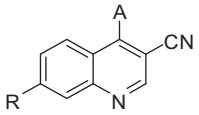

Compound	R	A	LRRK2 (wt) IC_{50} (μM)	LRRK2 (G2019S) IC_{50} (μM)	LRRK2 (G2019S) EC_{50} (μM)
6	4-(Methylsulfonyl)phenyl	Isopropylamino	0.032	0.028	0.435
14	1-Methyl-1*H*-pyrazol-4-yl	Isopropylamino	0.007	0.005	0.140
15	4-(*N*-Methylsulfamoyl)phenyl	Isopropylamino	0.009	0.006	0.226
16	4-(Morpholinosulfonyl)phenyl	Isopropylamino	0.014	0.010	0.416
17	2-Methylthiazol-5-yl	Isopropylamino	0.023	0.016	0.545
18	4-(Pyrrolidin-1-ylsulfonyl)phenyl	Isopropylamino	0.012	0.019	—
19	4-(*N*,*N*-Dimethylsulfamoyl)phenyl	Isopropylamino	0.037	0.028	—
20	6-(Methylsulfonyl)pyridin-3-yl	Isopropylamino	0.064	0.048	1.599
21	5-Chlorothiophen-2-yl	Isopropylamino	0.109	0.065	2.621
22	H	Isopropylamino	0.103	0.288	—
23	1-Methyl-1*H*-pyrazol-4-yl	Azetidin-1-yl	0.010	0.013	0.504
24	4-(Methylsulfonyl)phenyl	Azetidin-1-yl	0.016	0.014	—
25	4-(Methylsulfonyl)phenyl	Dimethylamino	0.020	0.027	1.134
26	4-(Methylsulfonyl)phenyl	Piperidin-1-yl	0.052	0.059	1.599
27	4-(Methylsulfonyl)phenyl	4-Methylpiperazin-1-yl	0.281	0.120	—
28	4-(Methylsulfonyl)phenyl	Methyl(phenyl)amino	0.450	0.278	—
29	4-(Methylsulfonyl)phenyl	Imidazol-1-yl	0.682	0.498	—
30	4-(Methylsulfonyl)phenyl	*N*-Methylacetamido	2.333	1.177	—
31	4-(Methylsulfonyl)phenyl	(*R*)-Cyclopropylethylamino	0.046	0.039	—
32	4-(2-Oxooxazolidin-3-yl)phenyl	(*R*)-Cyclopropylethylamino	0.048	0.027	0.731

Biochemical enzyme activity was determined using GST-LRRK2(970-2527), GST-(G2019S)LRRK2(970-2527), and LRRKtide in the presence of 100 μM ATP. Cellular activity was determined using HEK293 cells stably transfected with LRRK2 (G2019S).

Our cellular assay monitored Ser935 phosphorylation which is known to depend on LRRK2 kinase activity.[16] Good correlation between in vitro and cellular measures was observed. A correlation analysis of LRRK2 (G2019S) biochemical IC_{50}'s with cellular EC_{50}'s showed $R^2 = 0.88$. The most potent compound was **14** which registered a 140 nM EC_{50}.

We profiled compound **6**, **14**, and **32** against a panel of 40 kinases.[17] At a concentration of 1 μM, compound **14** inhibited the kinase activities of AURA, FLT3, PLK2 and SYK at greater than 80%. However, at 1 and 10 μM, respectively, neither compounds **6** nor **32** inhibited any kinases in the panel to such an extent. The highest inhibition observed with these compounds was against SYK (71% and 80%). These three compounds differ most greatly in their substitution at C7 and this observation suggests that inhibitor interactions with residues near the solvent channel might be exploited for improving LRRK2 selectivity.

We assessed the CNS exposure of compounds **6**, **14**, and **32** in both Mdr1 a/b (−/−) and P-gp competent wild-type FVB mice to obtain a measure of P-gp efflux and brain uptake. CNS penetration was observed at 5 min following a 1 mg/kg IV dose. Penetration was assessed from the brain to plasma concentration ratios (K_p) in the wild-type mice and was determined to be 0.7, 1.3, and 0.1 for compounds **6**, **14**, and **32** respectively. No significant P-gp efflux was observed and this was consistent with values obtained in vitro from MDR1-MDCK transfected cells.

Lead compound **14** was further evaluated in an in vivo pharmacodynamic study. BAC transgenic mice ($n = 5$ per group) expressing mouse LRRK2 with the human G2019S mutation were administered a single oral dose of compound **14** at 30 and 100 mg/kg.[18,19] Brain samples were collected at 3 h post dose and analyzed by sandwich ELISA to determine p-Ser935 and total LRRK2 levels.[20,21] Figure 2 shows that treatment with LRRK2 inhibitor **14** resulted in a significant reduction of the percent of phosphorylation at Ser935 at 30 and 100 mg/kg (30% and 44% reduction respectively, $^{*}p < 0.05$ and $^{***}p < 0.001$). Consistent with our observations

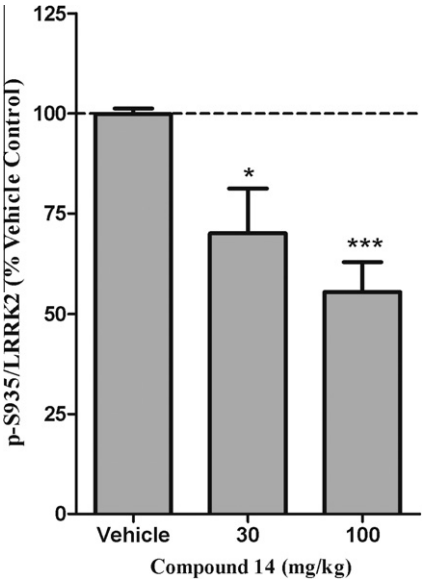

Figure 2. In vivo G2019S LRRK2 transgenic mouse pharmacodynamic study results. Transgenic mice were administered a single oral dose of compound **14** and brains were collected 3 h post dose for analysis. The p-Ser935 levels were determined by ELISA and normalized to total LRRK2. Data are expressed as the mean ratio of p-Ser935 to total LRRK2 normalized to values observed in the vehicle control group. Error bars represent SEM.

in FVB mice, we observed moderate CNS exposure of compound **14** in these transgenic animals. Brain to plasma concentration ratios were determined to be 1.2 at 30 mg/kg and 2.1 at 100 mg/kg.[22]

In summary, we have developed a series of 4-alkylamino-7-aryl-3-cyanoquinolines that inhibit LRRK2 kinase activity as measured in biochemical and cellular assays. Several compounds in this series were found to have high selectivity for LRRK2 inhibition

as measured in a panel of representative kinases. Compound **14** was dosed orally in an in vivo mouse model and found to significantly inhibit Ser935 phosphorylation at doses of 30 and 100 mg/kg in brain.

Acknowledgments

The authors thank Wayman Chan for performing difficult purifications. We would like to acknowledge the work of Pui Seto, Monica You, Jeanne Baker, and Kevin Tanaka for the production and purification of antibodies used in our assays. We also want to acknowledge Colin Lorentzen and Shawn Gauby for in vitro DMPK support and Pam Santiago for in vivo DMPK support. We also want to especially thank Dr. Takeshi Iwatsubo (University of Tokyo) for the generous gift of the HEK293 cell line stably expressing LRRK2-G2019S.

Supplementary data

Supplementary data associated with this article can be found, in the online version, at http://dx.doi.org/10.1016/j.bmcl.2013.02.041.

References and notes

1. Samii, A.; Nutt, J. G.; Ransom, B. R. *Lancet* **2004**, *363*, 1783.
2. de Lau, L. M. L.; Breteler, M. M. B. *Lancet Neurol.* **2006**, *5*, 525.
3. *National Institute of Neurological Disorders and Stroke*, National Institutes of Health. http://www.ninds.nih.gov/disorders/parkinsons_disease/parkinsons_disease_backgrounder.htm (accessed Feb 2013)
4. Rascol, O.; Payoux, P.; Ory, F.; Ferreira, J. J.; Brefel-Courbon, C.; Montastruc, J.-L. *Ann. Neurol.* **2003**, *53*, S3.
5. Zimprich, A.; Biskup, S.; Leitner, P.; Lichtner, P.; Farrer, M.; Lincoln, S.; Kachergus, J.; Hulihan, M.; Uitti, R. J.; Calne, D. B.; Stoessl, A. J.; Pfeiffer, R. F.; Patenge, N.; Carbajal, I. C.; Vieregge, P.; Asmus, F.; Müller-Myhsok, B.; Dickson, D. W.; Meitinger, T.; Strom, T. M.; Wszolek, Z. K.; Gasser, T. *Neuron* **2004**, *44*, 601.
6. Greggio, E.; Cookson, M. R. *ASN Neuro* **2009**, *1*, 13.
7. West, A. B.; Moore, D. J.; Biskup, S.; Bugayenko, A.; Smith, W. W.; Ross, C. A.; Dawson, V. L.; Dawson, T. M. *Proc. Natl. Acad. Sci. U.S.A.* **2005**, *102*, 16842.
8. Greggio, E.; Jain, S.; Kingsbury, A.; Bandopadhyay, R.; Lewis, P.; Kaganovich, A.; van der Brug, M. P.; Beilina, A.; Blackinton, J.; Thomas, K. J.; Ahmad, R.; Miller, D. W.; Kesavapany, S.; Singleton, A.; Lees, A.; Harvey, R. J.; Harvey, K.; Cookson, M. R. *Neurobiol. Dis.* **2006**, *23*, 329.
9. Jaleel, M.; Nichols, R. J.; Deak, M.; Campbell, D. G.; Gillardon, F.; Knebel, A.; Alessi, D. R. *Biochem. J.* **2007**, *405*, 307.
10. Detection was done using biotinylated LRRKtide, Eu(K)-Ab (p-Moesin)/SA-XL665 measured at 620 and 665 nm. GST-LRRK2 (aa970-2527) proteins containing either the wt sequence or a G2019S mutation were purchased from Life Technologies (Carlsbad, CA), and stored at −80 °C in small aliquots until use.
11. Scott, D. A.; Dakin, L. A.; Del Valle, D. J.; Diebold, R. B.; Drew, L.; Gero, T. W.; Ogoe, C. A.; Omer, C. A.; Repik, G.; Thakur, K.; Ye, Q.; Zheng, X. *Bioorg. Med. Chem. Lett.* **2011**, *21*, 1382.
12. Lunniss, C. J.; Cooper, A. W. J.; Eldred, C. D.; Kranz, M.; Lindvall, M.; Lucas, F. S.; Neu, M.; Preston, A. G. S.; Ranshaw, L. E.; Redgrave, A. J.; Robinson, J. E.; Shipley, T. J.; Solanke, Y. E.; Somers, D. O.; Wiseman, J. O. *Bioorg. Med. Chem. Lett.* **2009**, *19*, 1380.
13. Hudkins, R. L.; Diebold, J. L.; Tao, M.; Josef, K. A.; Park, C. H.; Angeles, T. S.; Aimone, L. D.; Husten, J.; Ator, M. A.; Meyer, S. L.; Holskin, B. P.; Durkin, J. T.; Fedorov, A. A.; Fedorov, E. V.; Almo, S. C.; Mathiasen, J. R.; Bozyczko-Coyne, D.; Saporito, M. S.; Scott, R. W.; Mallamo, J. P. *J. Med. Chem.* **2008**, *51*, 5680.
14. MLK1 (3DTC) was selected as the template for the homology model because its sequence was the closest human kinase domain in the pdb (BLAST score = 1*e*−25, with 31% identities). However, several features of the 3DTC structure indicate that it is an inactive conformation. The P-loop in 3DTC undergoes a ligand induced conformational change and the DFG sequence is partially disordered. The corresponding parts in our homology models were rebuilt using the structure of homologous kinases that were in the fully activated state.
15. Garofalo, A. W.; Adler, M.; Aubele, D. L.; Bowers, S.; Franzini, M.; Goldbach, E.; Lorentzen, C.; Neitz, R. J.; Probst, G. D.; Quinn, K. P.; Santiago, P.; Sham, H. L.; Tam, D.; Truong, A. P.; Ye, X. M.; Ren, Z. *Bioorg. Med. Chem. Lett.* **2013**, *23*, 71.
16. Dzamko, N.; Deak, M.; Hentati, F.; Reith, A. D.; Prescott, A. R.; Alessi, D. R.; Nichols, R. J. *Biochem. J.* **2010**, *430*, 405.
17. Compounds were profiled at Invitrogen in a single-point assay (see Supplementary data).
18. Li, X.; Patel, J. C.; Wang, J.; Avshalumov, M. V.; Nicholson, C.; Buxbaum, J. D.; Elder, G. A.; Rice, M. E.; Yue, Z. *J. Neurosci.* **2010**, *30*, 1788.
19. Breeding pairs were licensed from the Mt. Sinai School of Medicine.
20. An antibody recognizing the *N*-terminal region of LRRK2 (Elan Pharmaceuticals) was used for antigen capture, while another antibody against either LRRK2 (Elan Pharmaceuticals) or pSer935 (Epitomics) was used for detection. The data were normalized as a percentage of the vehicle-treated controls.
21. Our ELISA was calibrated by comparing results for a cross-section of LRRK2 inhibitors against Western blots. A linear correlation was observed with $R^2 = 0.82$. The correlation plot is included in the Supplementary data.
22. A table listing compound levels is included in the Supplementary data.